Publication Year	2022
Acceptance in OA	2025-03-17T14:12:39Z
Title	Spectral Rotational Characterization of the Didymos System prior to the DART Impact
Authors	IEVA, Simone, Epifani, E. Mazzotta, PERNA, Davide, DALL'ORA, Massimo, Petropoulou, V., Deshapriya, J. D.P., Hasselmann, P. H., ROSSI, Andrea, POGGIALI, Giovanni, BRUCATO, John Robert, PAJOLA, Maurizio, LUCCHETTI, Alice, IVANOVSKI, Stavro Lambrov, PALUMBO, Pasquale, DELLA CORTE, Vincenzo, Zinzi, A., Rivkin, A. S., Thomas, C. A., de León, J., Amoroso, M., Bertini, I., Capannolo, A., Cotugno, B., CREMONESE, Gabriele, Di Tana, V., Gai, I., Impresario, G., DOTTO, Elisabetta, Lavagna, M., MENEGHIN, Andrea, Miglioretti, F., Modenini, D., Pirrotta, S., SIMIONI, Emanuele, Simonetti, S., Tortora, P., Zannoni, M., Zanotti, G.
Publisher's version (DOI)	10.3847/PSJ/ac7f34
Handle	http://hdl.handle.net/20.500.12386/36861
Journal	THE PLANETARY SCIENCE JOURNAL
Volume	3

The Planetary Science Journal, 3:183 (8pp), 2022 August https://doi.org/10.3847/PSJ/ac7f34

Spectral Rotational Characterization of the Didymos System prior to the DART Impact*

Simone Ieva[1], E. Mazzotta Epifani[1], D. Perna[1], M. Dall'Ora[2], V. Petropoulou[1], J. D. P. Deshapriya[1], P. H. Hasselmann[1], A. Rossi[3], G. Poggiali[4,5], J. R. Brucato[4], M. Pajola[6], A. Lucchetti[6], S. L. Ivanovski[7], P. Palumbo[8,9], V. Della Corte[9], A. Zinzi[10,11], A. S. Rivkin[12], C. A. Thomas[13], J. de León[14,15], E. Dotto[1], M. Amoroso[10], I. Bertini[8], A. Capannolo[16], B. Cotugno[17], G. Cremonese[6], V. Di Tana[17], I. Gai[18], G. Impresario[10], M. Lavagna[16], A. Meneghin[4], F. Miglioretti[17], D. Modenini[18,19], S. Pirrotta[10], E. Simioni[6], S. Simonetti[17], P. Tortora[18,19], M. Zannoni[18,19], and G. Zanotti[16]
[1] INAF—Osservatorio Astronomico di Roma, Via Frascati 33, 00078, Monte Porzio Catone, RM, Italy; simone.ieva@inaf.it
[2] INAF—Osservatorio Astronomico di Capodimonte, Napoli, Italy
[3] Istituto di Fisica Applicata "Nello Carrara" (IFAC-CNR), Sesto Fiorentino, Firenze, Italy
[4] INAF—Osservatorio Astrofisico di Arcetri, Firenze, Italy
[5] LESIA—Observatoire de Paris, Université PSL, CNRS, Sorbonne Université, Université de Paris, France
[6] INAF—Osservatorio Astronomico di Padova, Padova, Italy
[7] INAF—Osservatorio Astronomico di Trieste, Trieste, Italy
[8] Universitá degli Studi di Napoli "Parthenope," Napoli, Italy
[9] INAF—Istituto di Astrofisica e Planetologia Spaziali, Rome, Italy
[10] Agenzia Spaziale Italiana (ASI), Rome, Italy
[11] Space Science Data Center—ASI, Rome, Italy
[12] JHU-APL, Laurel, MD, USA
[13] Northern Arizona University, Flagstaff, AZ, USA
[14] Instituto de Astrofísica de Canarias (IAC), Santa Cruz de Tenerife, Spain
[15] University of La Laguna, Department of Astrophysics, Santa Cruz de Tenerife, Spain
[16] Politecnico di Milano—Bovisa Campus, Dipartimento di Scienze e Tecnologie Aerospaziali, Milano, Italy
[17] Argotec, Torino, Italy
[18] Alma Mater Studiorum - Universitá di Bologna, Dipartimento di Ingegneria Industriale, Forlí, Italy
[19] Alma Mater Studiorum - Universitá di Bologna, Centro Interdipartimentale di Ricerca Industriale Aerospaziale, Forlí, Italy
Received 2022 February 7; revised 2022 May 19; accepted 2022 July 5; published 2022 August 3

Abstract

The smallest member of the Didymos binary near-Earth object system (Dimorphos) is the target of the DART/LICIACube mission, the first attempt to change the orbit of another celestial body via a kinetic impactor. It is important to characterize the unperturbed system prior to the DART impact. In this work we obtained, for the first time, spectral characterization of the system at several rotational phases from TNG+DOLORES in the visible range (0.34–0.81 μm). This is crucial in order to disentangle the primary and secondary bodies and highlight eventual dishomogeneities on their surfaces. We confirm that a subtle but persistent spectral variability appears, even when compared with data obtained from previous 2003 and 2019 apparitions. While the reason for such variability is still under investigation, our analysis hints that different compositions could play a role. Future observations during the brighter 2022 apparition in synergy with data obtained from LUKE on board LICIACube will definitely tackle this conundrum.

Unified Astronomy Thesaurus concepts: Near-Earth objects (1092); Ground telescopes (687); Spectrometers (1554)

1. Introduction

The identification of multiple systems among the near-Earth object (NEO) population has grown considerably in recent years, mostly due to the increasing use of radar observations and photometric lightcurves in NEO characterization. Recent studies estimate that nearly 15% of NEOs larger than 200 m should be binaries (Margot et al. 2015). Up to now, we know of the existence of at least 50 multiple systems (Margot et al. 2015; Monteiro et al. 2021), and even two triple NEOs (Brozović et al. 2011; Becker et al. 2015). Radar has proven to be a powerful method of detecting binary NEOs, enabling the discovery of secondary NEOs in 72% of the cases, while photometric measurements have been used to detect the remaining 28%. Overall, almost one in six NEOs should belong in a multiple system (Taylor 2012).

Binary NEOs have therefore attracted space agencies and private investors since they can help maximize the scientific return of a mission, essentially doubling the number of bodies visited and enabling scientific investigations of two small bodies , thus reducing the overall costs. Moreover, the study of binary bodies can also help shed light on binary formation. The most current explanation involves the reaccumulation of a body following a rotational disruption, probably as a result of the Yarkovsky–O'Keefe–Radzievskii–Paddack (YORP) effect (Pravec & Harris 2007; Walsh & Jacobson 2015). However, other mechanisms are predicted for different sizes and

* Based on observations made with the Italian Telescopio Nazionale Galileo (TNG) operated on the island of La Palma by the Fundación Galileo Galilei of the Istituto Nazionale di Astrofisica (INAF) at the Spanish Observatorio del Roque de los Muchachos of the Instituto de Astrofisica de Canarias (Program AOT42-TAC8).

populations of small bodies, like capture, collision and tidal processes (Margot et al. 2015; Walsh & Jacobson 2015).

65803 Didymos (1996 GT), discovered by the Spacewatch survey at Kitt Peak observatory in 1996, is a very interesting NEO. Hints of its binarity first arose in Goldstone radar observations, and were later confirmed with optical lightcurve analysis, along with Arecibo radar imaging in 2003 (Pravec et al. 2003). Radar and lightcurve data have established a diameter of 780 ± 80 m, with a well-known rotational period of $2.259\,3 \pm 0.0002$ hr, for the primary (Didymos), while the secondary, later renamed Dimorphos, has a projected diameter of 163 ± 18 m and an orbital period of 11.920 ± 0.005 hr (Pravec et al. 2022). The study of the rotational properties of the system are even more crucial due to the fact that Didymos belongs to a rare class of binaries whose primary is at risk of rotational disruption (Walsh et al. 2008). Regarding its dynamical origin in the main belt, Richardson et al. (2016) suggested that Didymos has a likely chance (>82%) to have reached its current orbit by exiting the inner main belt, near or within the ν_6 resonance, located between 2.1 and 2.5 au.

Few spectroscopic observations of the Didymos system have been taken during its previous apparitions of 2003 and 2019. Nonetheless, its physical characterization has been puzzling. Binzel et al. (2004) originally taxonomically classified the system as an Xk-type using visible data. Later, de León et al. (2006, 2010) extended its taxonomy in the near-IR (NIR) range and classified it as a potential S-type asteroid. Dunn et al. (2013) confirmed that it is spectroscopically most consistent with ordinary chondrites, with an affinity for L/LL-type meteorites. Nowadays there is a general consensus on its silicate composition, while few anomalies still remain. For instance, its 2 μm band appears shallower than the typical silicate type (see also Michel et al. 2016).

The scientific interest in the Didymos system has increased in recent years due to the fact that it has been selected as the target of the NASA Double Asteroid Redirection Test (DART; Rivkin et al. 2021) and Hera (Michel et al. 2022) missions. DART will be the first mission to demonstrate the applicability of the kinetic impactor method for planetary defense (Cheng et al. 2018). After being launched on 2021 November 23, the DART spacecraft will impact the smallest member of the Didymos binary asteroid on 2022 September 26. The ASI Light Italian Cubesat for Imaging of Asteroid (LICIACube, Dotto et al. 2021) will piggyback on the DART mission. The 6U CubeSat will be released in the proximity of the target and will perform an autonomous fly-by of the Didymos system, probing the DART impact and reaching several scientific goals, such as testifying the impact of DART, studying the structure and evolution of the ejecta plume, and characterize the nonimpacted hemisphere. The Hera mission, to be launched in late 2024, will measure in great detail the outcome of NASA's DART mission kinetic impactor test. Hera will also conduct a detailed study of both asteroids, carrying onboard scientific payloads including a framing camera and a hyperspectral imager.

Apart from the planetary defense demonstration, which will be the main purpose of DART, this space mission will provide a unique opportunity to study binary asteroids and deepen our knowledge on the origins and evolution of the solar system. It is clear that in order to provide the proper interpretational context of the Didymos system prior to the arrival of DART and LICIACube, it is crucial to obtain a detailed characterization for the surface of the system prior to the impact. To achieve this purpose, in the framework of a larger observational campaign aimed at the characterization of the Didymos system prior to the DART visit, we obtained for the first time a spectral characterization of the Didymos system at several rotational phases during its brightest peak in the 2021 apparition ($V = 18.9$). The data obtained in this work will also be of paramount importance for the Hera mission, which will carry an hyperspectral imager whose wavelength range overlaps with the spectra obtained in this study.

2. Observations and Data Reduction

Observations were carried out at the 3.6 m Telescopio Nazionale Galileo (TNG, La Palma, Spain) during two separate runs in 2021 February. Visible spectroscopy was performed with the DOLORES (Device Optimized for the LOw RESolution) instrument, a low-resolution spectrograph and camera permanently installed at the Nasmyth B focus of the TNG. The camera is equipped with a 2048×2048 E2V 4240 thinned back-illuminated, deep-depleted, Astro-BB coated CCD with a field of view of $8\farcm6 \times 8\farcm6$ and a $0\farcs252$ pix^{-1} scale. Observations were performed with the low-resolution blue grism (0.34–0.81 μm spectral range, $R = 585$).

Spectra for Didymos and several solar analogs were obtained using the same configuration: through a 2″ slit oriented along the parallactic angle (i.e., the angle at which the slit is aligned with the direction from the target to the zenith). This is important when observing targets away from the zenith, since the light is dispersed in the vertical direction as a result of atmospheric differential refraction, and certain wavelengths could fall outside the slit, resulting in an incomplete spectrum. Spectra were reduced with the ESO-MIDAS software package using standard procedures (e.g., see Ieva et al. 2018): bias subtraction from the raw data and flat-field correction, cosmic-ray removal, background subtraction, collapsing the two-dimensional spectra into one dimension, wavelength calibration (using Ar and Ne+Hg lamp emission lines), and atmospheric extinction correction. Spectra were all normalized at 0.55 μm. The reflectivity for the Didymos spectra was then obtained by dividing its spectra by one of the solar analogs observed during the night. Since changes in the sky conditions have an effect on the reflectance spectra, we favored solar analogs that have a similar airmass compared to the Didymos spectrum, and preferentially obtained close in time. The circumstances are given in Table 1. Final spectra are reported in Figure 1.

3. Results

3.1. Visible Spectral Slope Variation and Comparison with Available Spectra

In Figure 1 we reported our observed reflectance spectra, smoothed around a 5 pixel boxcar. We collected a total of eight spectra, seven distributed during the night of 2021 February 15, and another one obtained during the night of February 23 (see also Table 1). From Figure 1 it is possible to see that all of the spectra retrieved by our group are very similar, with a spectral behavior slightly redder for the three spectra acquired during the first part of the night of February 15 (spectra ids #1, #2, and #3), and slightly flatter spectra obtained during the second part of the night (spectra ids #4, #5, #6, and #7). The only spectrum obtained during the night of February 23 (id #8) shows a spectral behavior somewhat in between.

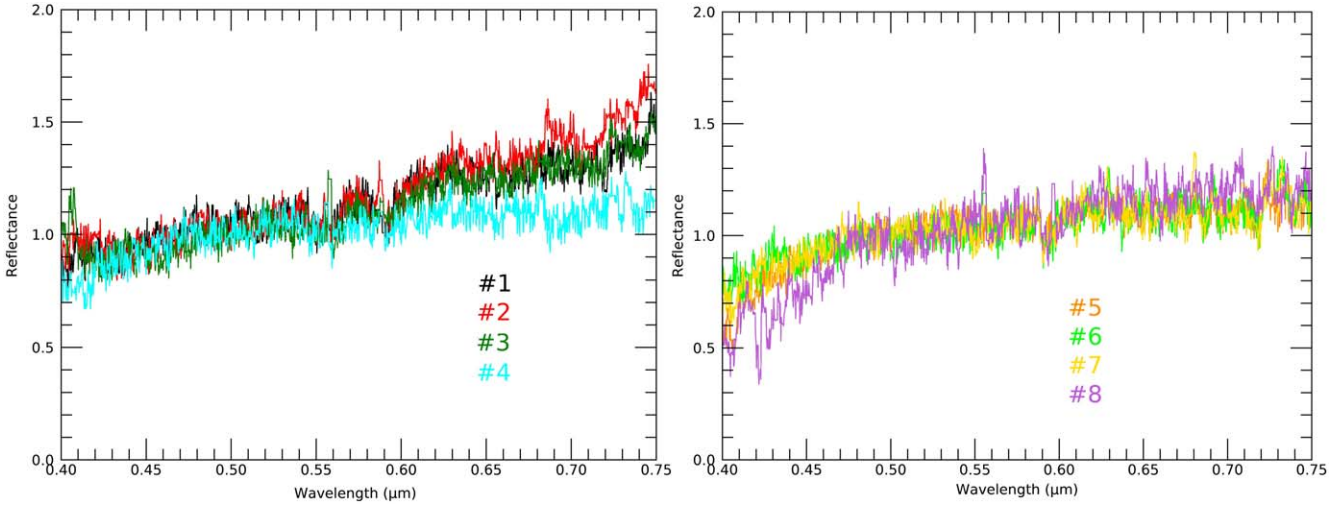

Figure 1. All the spectra observed in the 2021 apparition from TNG. Spectra 1–7 were observed on the night of February 15, while spectrum 8 was observed on February 23. All spectra are normalized at 0.55 μm.

Table 1
Observational Circumstances for the Spectra Observed at TNG during the 2021 February Runs Together with the Same Values Retrieved for Other Spectra Obtained in Previous Apparitions

Spectrum ID	Telescope	Date	UT Start/End	Exp. Time (s)	Airmass	Δ (au)	r (au)	α (deg)	Solar Analog
BIN04	PALOMAR	06/03/02	06:46–07:33	2700	1.022–1.057	1.21	2.15	15.4	...
JDL10	NOT	16/01/04	00:27–00:52	1440	1.039–1.080	0.33	1.28	22.8	...
JDL19	GTC	17/04/19	21:08–22:09	3 × 1200	1.110–1.055	1.26	2.09	19.9	...
#SA1	TNG	16/02/21	00:20–00:21	15	1.321	...	...	...	...
#1	TNG	16/02/21	01:19–01:49	1800	1.040–1.023	1.12	2.10	5.8	#SA2
#2	TNG	16/02/21	01:58–02:28	1800	1.200–1.206	1.12	2.10	5.8	#SA3
#3	TNG	16/02/21	02:40–03:10	1800	1.030–1.050	1.12	2.10	5.8	#SA3
#4	TNG	16/02/21	03:18–03:48	1800	1.066–1.114	1.12	2.10	5.8	#SA2
#5	TNG	16/02/21	03:57–04:27	1800	1.135–1.215	1.12	2.10	5.8	#SA2
#6	TNG	16/02/21	04:39–05:01	1320	1.249–1.328	1.12	2.10	5.8	#SA1
#7	TNG	16/02/21	05:47–06:17	1800	1.628–1.920	1.12	2.10	5.7	#SA1
#SA2	TNG	16/02/21	05:26–05:28	10	1.124	...	...	...	...
#SA3	TNG	16/02/21	06:28	10	1.034	...	...	...	...
#8	TNG	24/02/21	03:15–03:45	1800	1.193–1.298	1.16	2.14	5.2	#SA4
#SA4	TNG	24/02/21	04:56	10	1.251	...	...	...	...

Note. The columns show the date, start/end time, exposure time, airmass, topocentric (Δ) and heliocentric (r) distance, and phase angle (α). BIN04 obtained from Binzel et al. (2004), JDL10 appeared in de León et al. (2006, 2010), and JDL19 retrieved by personal communication. Solar analogs are SA98-978 (#SA1), HD144873 (#SA2 and #SA3) and SA107-684 (#SA4).

The Didymos system has been extensively investigated during the previous passages of 2003 and 2019 (Pravec et al. 2003; de León et al. 2010). However, a very limited number of optical and near-infrared spectra have been published, mostly because of its faint nature during previous passages. In Figure 2 we report three representative spectra collected in this work (#1, #5, and #8), together with data retrieved from the literature (Binzel et al. 2004; de León et al. 2010, hereafter BIN04 and JDL10, respectively) and obtained by private communication (J. de León 2019; JDL19). Our data, collected for the first time at several rotational phases, confirmed its overall silicate nature, although some variability still appears. It is possible to see in Figure 2 that the first group of spectra (ids #1–#3) should be more similar to the one obtained by de León in the 2019 passage (JDL19), while the BIN04 spectrum is more akin to spectra presented in this work and obtained during the second part of the night (ids #4–#7). Incidentally, the only spectrum acquired during the night of February 23 (#8) shows an intermediate slope between the two groups, and an affinity with JDL10 data.

In order to quantify spectral differences among data obtained at different epochs, we decided to compute the normalized reflectance slope in the 0.5–0.7 μm wavelength range, in units of %/0.1 μm, following the Luu & Jewitt (1990) approach, as:

$$S = (dS/d\lambda)/R_{0.55}, \quad (1)$$

where $R_{0.55}$ is the reflectance at 0.55 μm. Final values for the 0.5–0.7 μm slope are reported in Table 2 for all the spectra considered in this work. It is important to stress that comparing reflectance slopes for spectra obtained weeks, or even years, apart is not easy, since spectral slopes are influenced also by observational conditions, like viewing geometry, the phase

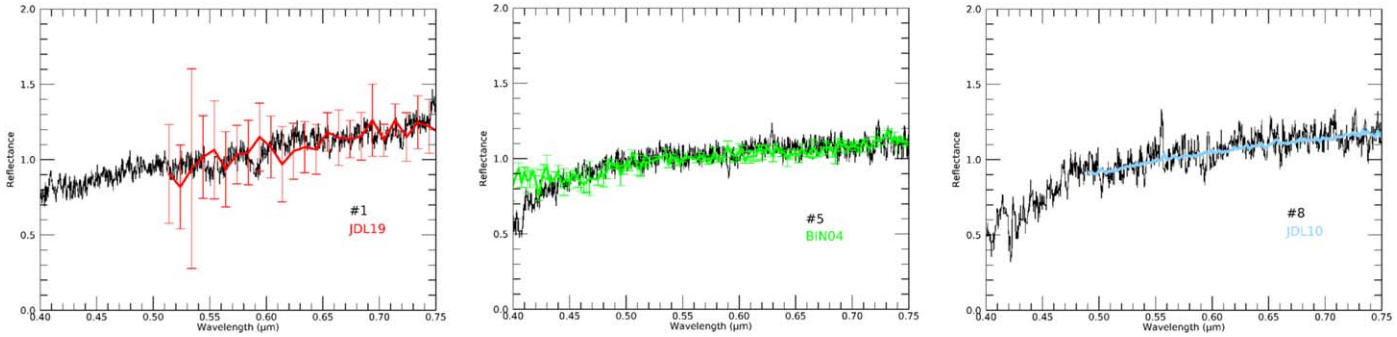

Figure 2. Comparison between a representative set of spectra collected during our observations in 2021 (#1, #5, and #8) together with previously observed spectra of the Didymos system retrieved from the literature. (Left) Spectrum #1 together with the one observed by J. de León in 2019 in red (JDL19). (Middle) #5 together with one from Binzel et al. (2004) in green. (Right) spectrum #8 with one retrieved by de León et al. (2010) in cyan.

angle, and also by physical reddening mechanisms (i.e., space weathering). However, spectral-reddening effects due to the phase angle among silicate bodies start to appear from $\alpha > 25°$ (see Reddy et al. 2015) and our phase-angle range (Table 1) is similar and always below that threshold value. Furthermore, to cope with intrinsic spectral variations due to different observational conditions (e.g., the use of different solar analogs) as an ulterior error bar we added the median absolute deviation among slopes computed for the same spectrum using different solar analogs. Nonetheless, all solar analogs show a very similar spectrum.

Spectra obtained during the first part of the night (#1–#3) show a steeper slope, with S varying between 13.65 and 20.02%/0.1 μm, while the second part of the night (spectra #4–#7) is characterized by a flatter and more homogeneous slope, with S between 4.40% and 6.57%/0.1 μm. Moreover, the JDL19 spectrum shows a slope of $S = 16.05\% \pm 2.55\%/0.1$ um, similar to the first group, while the BIN04 spectrum available on the SMASS[20] database shows a slope ($S = 5.13\% \pm 0.51\%/0.1\ \mu$m) more in tune with the second group. Finally, the JDL10 spectrum shows an intermediate slope between the two groups, with $S = 11.21\% \pm 0.22\%/0.1\ \mu$m, similar to the spectral slope derived for the only spectrum observed during the night of February 23 (id #8). This quantitatively confirms similarities between our observed spectra and previously collected data.

3.2. Spectral Variations among Mutual Events

For a binary system, mutual events, namely occultations and eclipses of the primary or the secondary body, can occur during the observational slot. At the moment of our observations the dynamic solutions for the Didymos system were not known with a good-enough accuracy, and we were left with three potential solutions for each mutual event. Nonetheless, we managed to observe at least one full event, in order to ideally disentangle the contribution of the primary and secondary asteroids, and look for potential similarities and differences between the two bodies.

After the 2021 photometric observational campaign (Pravec et al. 2022) we were left with only one solution for each mutual event. Using a helpful lookup table available on the DART Observation WG repository,[21] we identified mutual events that occurred during our observational timeframe. We managed to observe the primary eclipse twice, during the nights of February 15 and February 23. Spectral slopes are reported in Figure 3 according to their Julian date. It is possible to see that spectra #4–#7 encompass the primary eclipse event, with spectrum #4 taken just before the beginning of the eclipse and spectrum #7 just after the end of the event. The analysis of those spectral slopes shows a substantial similarity of the spectral behavior before and after the beginning and the end of the primary eclipse, suggesting a potential similarity of the primary and secondary bodies. Spectrum #8 also corresponds to a primary eclipse (Figure 3) showing, however, a slightly larger spectral slope, possibly connected to the sampling of a different location (see Section 3.3).

Table 2
Spectral Slope, Computed in the 0.5–0.7 μm Range, together with the Primary Rotational Phase for all Spectra Considered in this Work

Spectrum ID	Spectral Slope (%/0.1 μm)	Primary Rotational Phase
BIN04	5.13 ± 0.51	...
JDL10	11.21 ± 0.22	...
JDL19	16.05 ± 2.55	...
#1	13.65 ± 1.14	0.000 ± 0.110
#2	20.02 ± 1.17	0.288 ± 0.110
#3	16.34 ± 1.08	0.598 ± 0.110
#4	4.40 ± 1.08	0.878 ± 0.110
#5	5.43 ± 0.96	0.166 ± 0.110
#6	6.57 ± 1.20	0.446 ± 0.081
#7	5.30 ± 1.20	0.977 ± 0.110
#8	12.55 ± 1.44	0.838 ± 0.110

Note. Rotational phase was determined by conventionally assigning a phase 0 to the first spectrum acquired (#1), and computing the number of fractional periods between #1 and the other data. Due to the extreme accuracy achieved for the Didymos rotational period in the 2021 campaign, spectrum #8, obtained 8 days later than #1–#7, has an additional uncertainty of 0.7%. For BIN04, JDL10, and JDL19 no rotational phase was computed, since the large distance in time between these data and our spectra translates in a large final uncertainty.

3.3. Rotational Variation

Spectral variability observed among different data sets for Didymos can also be related in principle to rotational variation, i.e., the fact that we are observing from Earth different disk-integrated portions of the asteroid surface. However, it is tricky

[20] http://smass.mit.edu/catalog.php
[21] https://sites.google.com/view/didymosobs/tools?authuser=0

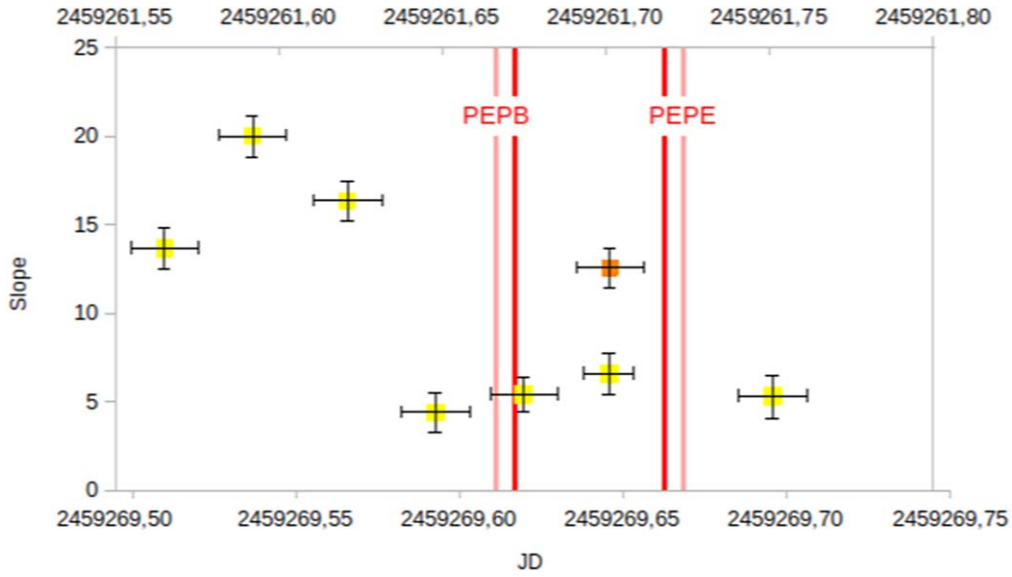

Figure 3. Spectral slopes for spectra observed during the night of 2021 February 15 (in yellow) and February 23 (in orange) alongside their Julian date (JD). We show JD computed for the first night below the same quantity for the second night. We also remark in red the beginning and end of the only mutual event observed during the nights, the primary eclipse. In light red we report the current uncertainty on the occurrence of the event (±8 minutes).

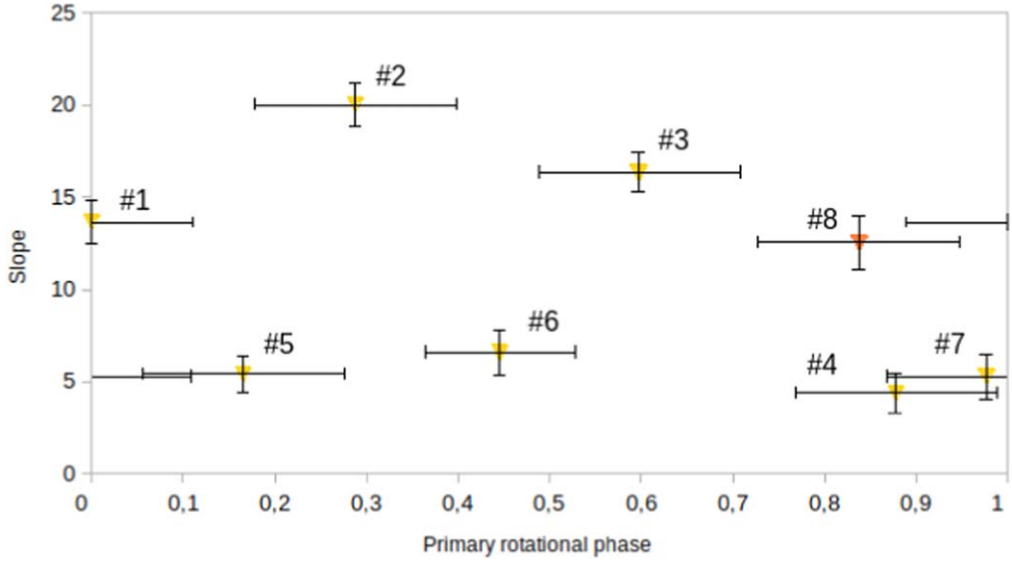

Figure 4. Spectral slopes computed for the 2021 data set considered in this work vs. the fractional rotational phase, assigned based on the primary lightcurve. For simplicity, 0 is assigned to the first spectrum available (#1). Spectra acquired during the nights of February 15 and February 23 are represented in yellow and orange, respectively.

to compare spectra obtained in different conditions and reduced by different observers, especially for spectra characterized during different oppositions. Indeed, while in principle the rotational phase can be determined even for older spectra of the Didymos system, the large separation in time between these data and spectra obtained in this work translates into a large uncertainty of the final rotational phase. Therefore, we choose to consider only spectra observed in 2021. Our spectroscopic follow-up, using an homogeneous set of observations collected and reduced by the same team, confirmed that a potential regional variability exists (e.g., see Perna et al. 2015).

The Didymos rotation period is extremely well known after the 2021 observational campaign ($T = 2.2593 \pm 0.0002$, Pravec et al. 2022). Therefore, it is possible to assign to each spectrum a rotational phase, corresponding to spectra obtained at different phases of its lightcurve. For simplicity, we assigned a rotational phase 0 to the first spectrum available (#1) and computed the number of fractional periods occurring between #1 and other spectra. Due to the extreme accuracy achieved for the Didymos rotational period in the 2021 campaign spectrum #8, obtained 8 days later than #1–#7, has an additional uncertainty of 0.7%. Final rotational phases are reported in Table 2 and in Figure 4. Central points represent the rotational phase computed at the middle of spectral observations, while error bars account for the time range (UT start/end) of each single exposure.

It is possible to see that, although some variability still remains, we have a good agreement between spectra #4, #5, and #7. This data, observed a few hours apart and with a similar spectral slope, could be sampling adjacent regions on Didymos, (considering that the 2″ slit width corresponds to 8 pixels on the CCD, i.e., one-quarter of Didymos's observable surface). We also notice an agreement between #1 and #8. In

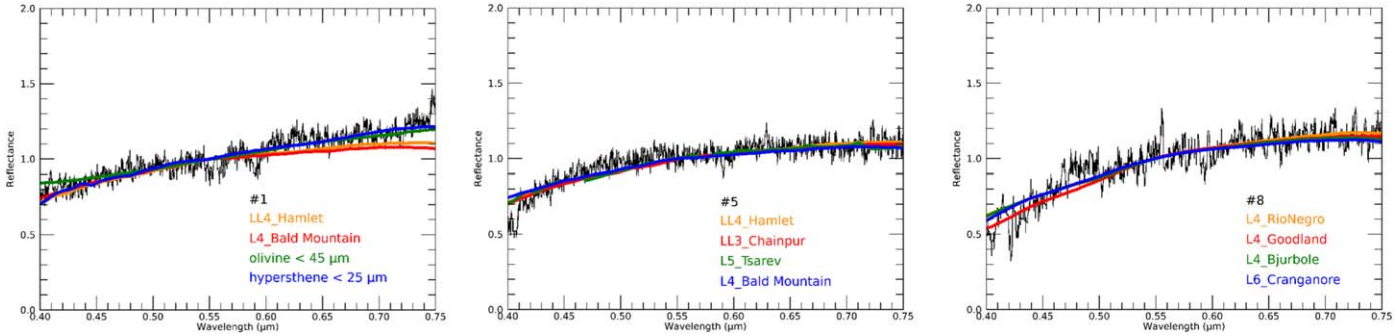

Figure 5. Comparison between three representative Didymos spectra observed at TNG during the 2021 observational window (#1, #5 and #8) with their best meteorite analog, selected among the 50 best fits retrieved using the M4AST tool. The tool was used to compare our data with the whole RELAB database, selecting the ones with a lower χ^2 value that better mimic the overall spectral behavior.

this case, while spectra were taken 8 days apart, the geometry is very similar and it is plausible that we could be sampling a similar region. At the same time, spectra #1 and #7 raise some concern with this interpretation, since they should insist on a similar region but they show a larger slope variation. This could be related to the fact that all these spectra are actually disk integrated, or less likely to vary in the observing conditions (i.e., airmass) between beginning and end of the night.

3.4. Comparison with RELAB Database

We investigated the suitable meteorite analog type for the system by comparing the observed reflectance spectra with laboratory reflectance spectra of meteorites. Such a comparison presents some limitations (see Binzel et al. 2015). For example, it is known that some spectral variation can arise between ground-based data and laboratory spectra, which are usually obtained at room temperature and pressure, while asteroids experience a whole range of different temperatures in vacuum. Nevertheless, these effects generally produce a variation of the position and the depth of the absorption features (Moroz et al. 2000; Poggiali et al. 2021), and have very weak effects on the spectral slope, which can be considered a diagnostic for suitable meteorite comparison. Spectral slopes can be influenced by space weathering, which generally on silicate material has the net effect of increasing the spectral slope (reddening). To take this into account, the RELAB database also contains sample spectra of irradiated meteorites/analogs. All these considerations make us confident that this kind of comparison is suitable to obtain an indication of the composition of the asteroid surface.

Using the M4AST online tool (Popescu et al. 2012) and a χ^2 minimization method, we compared three of our observed spectra (#1, #5, and #8) with the whole sample of >24,000 meteorite spectra included in the RELAB database (Milliken et al. 2016). We preferred to not make any a priori selection on the meteorite spectra to be used for comparison with Didymos data (e.g., ordinary chondrite meteorites, usually the best analog for silicate material), but we chose the first 50 fits with the lowest χ^2 value given by the tool. Among these, to identify a suitable meteorite analog, we took into consideration the meteorite spectrum that was also able to better reproduce the overall spectral behavior of the asteroid spectrum.

The best meteorite matches are reported in Figure 5. Spectrum #1, representing the ones with a steeper slope (together with #2 and #3) shows a general similarity with silicate material, although multiple assemblages present on the RELAB database could potentially be a good match. The best analog ideally could be found in a hypersthene with a grain size <25 μm, or possibly olivine with a grain size <45 μm, the principal components of L-chondrite meteorites. A comparison with L and LL ordinary chondrites however still seems pretty good, although these meteorites, considered the best analog for Didymos (Dunn et al. 2013) have a lower reflectance starting from 0.6 μm. For spectrum #5 we suggest a possible meteorite analog, characterized by a low χ^2 value and an overall good-quality fit, either an L or a LL ordinary chondrite, which are the meteorites that better fit the overall spectral behavior. Finally, for spectrum #8 we ended up with only L-chondrite meteorites with similar χ^2 values that can therefore be considered the most suitable spectral analogs.

In general we can confirm the results of Dunn et al. (2013), that using a larger wavelength range and laboratory-calibrated relations suggest an ideal comparison for Didymos of either L- or LL- ordinary chondrites. Spectra #1–#3 can also be compatible with either hypersthene or olivine because of their higher reflectance slope after 0.6 μm compared to ordinary chondrites. To confirm this result, NIR spectroscopic characterization is needed.

4. Discussion

Our overall analysis shows a potential subtle but persistent variation of the spectral slope on the Didymos system, computed in our case between 0.5 and 0.7 μm. Indeed, based only on spectra acquired during the 2021 opposition, there is a noticeable difference between spectra acquired at the beginning of the night of February 15, (more steep, with a spectral slope $S > 13\%/0.1$ μm) compared with others acquired later in the night showing a more flattish behavior ($S < 7\%/0.1$ μm). The only spectrum obtained during the night of February 23 shows a slope in between the two groups.

While the subtle variations in principle could be due to the contribution of the secondary body, it is known that Dimorphos, being roughly one-fifth of Didymos diameter, should contribute only 4% of the light, assuming a similar albedo and composition of the primary. Any differences in spectral behavior eventually present should be enormous to be noted at this stage, particularly because the system was very faint ($V = 18.9$). However, the second group of spectra (id #4–#7) obtained during the night of February 15 encompass a mutual event, namely a primary eclipse. These spectra acquired right before, during, and right after the event show a

remarkably homogeneous slope, potentially indicating a similarity of the primary/secondary body. This indication, and the fact that the contribution of Dimorphos for these spectra should be very minimal, due to the overall faintness of the system, could eventually mean that differences in spectral behavior we see at the moment are not due to inhomogeneities of the secondary with respect to the primary body.

It is also possible that spectral variation could be due to different observational conditions (different viewing geometries, e.g., phase angle, aspect angle...). However, all of the spectra presented on this work and acquired in 2021 were retrieved during the same night, or at worst 8 days later, thus having the same or a very similar viewing geometry. While it is difficult to compare spectral data sets obtained from different oppositions, it is worth noticing that spectra #1–#3 are more similar to JDL19, while spectra #4–#7 look mostly like BIN04 and #8 is akin to JDL10. In principle, to remove the ambiguity due to different geometries we could compare rotational phases for all data involved in the data set. However, while the rotational period is extremely well known, the large separation in time between spectra acquired 2 and 17 years before our data translates into a large final uncertainty. Therefore, in our work we were limited to the 2021 spectra.

Our analysis shows that some spectra having a similar slope could potentially look at a similar region on the surface of Didymos, taken hours (#4, #5, and #7), and even days (#1 and #8) apart. On the contrary, some spectra, centered at a similar rotational phase, show instead a larger variation in spectral slope (see, e.g., #1 and #7). It is important to remember that these ground-based observations are disk integrated, which cannot exclude the presence of small extended and/or localized surface variegations.

Spectral variability can have a physical explanation (different composition, space weathering). Hints for this solution can be found in our comparison with spectra of meteorites and minerals retrieved from the RELAB database. While spectra #4–#8 show an affinity with either L or LL ordinary chondrites, confirming the indirect results of Dunn et al. (2013), spectra #1–#3 has multiple potential matches, showing similarities with ordinary chondrites, either from pure spectra of hypersthene and olivine, the principal components found in L ordinary chondrites. This could indirectly indicate that different regions on Didymos's surface show a local variation on hypersthene and olivine concentrations, with some portions richer in those silicates, while others are more similar to L-chondrite assemblages. While new spectral characterization, ideally in the 2022 apparition (when the system will be brighter than in the last two decades) is required to confirm these interesting results, RGB images obtained by LUKE on board LICIACube (Poggiali et al. 2022) would definitely resolve this conundrum.

5. Summary and Conclusions

We obtained a new spectroscopic characterization of the Didymos system during the 2021 apparition, for the first time at different rotational phases.

1. Spectra acquired in 2021 show an intrinsic subtle, but persistent, variability, as testified by our analysis of the visible spectral slope between 0.5–0.7 μm. Spectra #1–#3, acquired at the beginning of the night of February 15, show a steeper slope respect to others (#4–#7). Spectrum #8, obtained 8 days apart, shows an intermediate similar slope.
2. Comparison with the few available literature data confirms a persistent variability, with data observed by Binzel et al. (2004) similar to the flattish #4–#7 spectra, while data observed by J. de León in 2019 is more similar to #1–#3; #8 seems to be more in tune with data retrieved from de León et al. (2010).
3. We observed one mutual event, a primary eclipse. Spectra #4–#7, which completely encompass this event, are very similar, suggesting a similarity between primary and secondary body. However, this must be taken cum grano salis, since the smaller dimension of Dimorphos suggests that it should contribute only 4% of the light.
4. To potentially identify source regions for each spectrum on the surface of Didymos, we assign a rotational phase to each of the spectra acquired in 2021. While it is possible that spectra with a similar slope taken during the same night (#4 and #7) and 8 days apart (#1 and #8) are related to similar regions of Didymos's surface, some incongruities (e.g., spectra #1 versus #7) complicate such a picture. However, our disk-integrated observations cannot exclude the presence of local-scale heterogeneity.
5. Comparison with the RELAB database confirms a general similarity between Didymos and the L/LL ordinary chondrites. However, steeper spectra can also be composed of hypersthene/olivine, the major components of L-chondrites.

All this could suggest that the different spectral behavior is probably connected to slightly different concentrations of olivine and hypersthene, as indicated by our comparison with laboratory data. At the moment, the causes for such discrepancies are not known. This could point out the presence of some local heterogeneities on either the surface of Didymos, Dimorphos, or both. However, even this explanation presents some concerns. It is best to admit at this stage that our knowledge of the Didymos system is incomplete. The causes for such spectral variation will likely be resolved thanks to high-resolution images captured by instruments on board the DART/LICIACube mission. In the meantime, new spectroscopic characterization, ideally in the NIR range (where the system has an anomalous spectroscopic behavior), and acquired during the 2022 closest approach, when Didymos will be brighter than in the last two decades, will be helpful to unveil this fascinating conundrum.

This research was supported by the Italian Space Agency (ASI) within the LICIACube project (ASI-INAF agreement AC No. 2019-31-HH.0). This work is based on observations made with the Italian Telescopio Nazionale Galileo (TNG) operated on the island of La Palma by the Fundación Galileo Galilei of the Istituto Nazionale di Astrofisica (INAF) at the Spanish Observatorio del Roque de los Muchachos of the Instituto de Astrofisica de Canarias (Program AOT42-TAC8).

We would like to thank J. de León for providing us with the spectrum acquired during the 2019 apparition.

Facilities: TNG(DOLORES).

ORCID iDs

Simone Ieva https://orcid.org/0000-0001-8694-9038
E. Mazzotta Epifani https://orcid.org/0000-0003-1412-0946
D. Perna https://orcid.org/0000-0002-4545-3850

M. Dall'Ora https://orcid.org/0000-0001-8209-0449
J. D. P. Deshapriya https://orcid.org/0000-0002-5758-1286
P. H. Hasselmann https://orcid.org/0000-0003-1193-8945
A. Rossi https://orcid.org/0000-0001-9311-2869
G. Poggiali https://orcid.org/0000-0002-3239-1697
J. R. Brucato https://orcid.org/0000-0002-4738-5521
M. Pajola https://orcid.org/0000-0002-3144-1277
A. Lucchetti https://orcid.org/0000-0001-7413-3058
S. L. Ivanovski https://orcid.org/0000-0002-8068-7695
P. Palumbo https://orcid.org/0000-0003-2323-9228
V. Della Corte https://orcid.org/0000-0001-6461-5803
A. Zinzi https://orcid.org/0000-0001-5263-5348
A. S. Rivkin https://orcid.org/0000-0002-9939-9976
C. A. Thomas https://orcid.org/0000-0003-3091-5757
J. de León https://orcid.org/0000-0002-0696-0411
E. Dotto https://orcid.org/0000-0002-9335-1656
M. Amoroso https://orcid.org/0000-0003-2603-165X
I. Bertini https://orcid.org/0000-0002-0616-2444
A. Capannolo https://orcid.org/0000-0002-4917-287X
B. Cotugno https://orcid.org/0000-0003-3868-8819
G. Cremonese https://orcid.org/0000-0001-9021-1140
I. Gai https://orcid.org/0000-0002-5367-3650
G. Impresario https://orcid.org/0000-0001-8984-4231
M. Lavagna https://orcid.org/0000-0003-4361-1437
A. Meneghin https://orcid.org/0000-0003-1665-6664
D. Modenini https://orcid.org/0000-0002-1517-3938
S. Pirrotta https://orcid.org/0000-0003-0377-8937
E. Simioni https://orcid.org/0000-0001-5993-0868
S. Simonetti https://orcid.org/0000-0002-1309-2958
P. Tortora https://orcid.org/0000-0001-9259-7673
M. Zannoni https://orcid.org/0000-0002-4151-9656
G. Zanotti https://orcid.org/0000-0002-3157-7588

References

Becker, T. M., Howell, E. S., Nolan, M. C., et al. 2015, Icar, 248, 499
Binzel, R. P., Reddy, V., & Dunn, T. L. 2015, in Asteroids IV, ed. P. Michel, F. E. DeMeo, & W. F. Bottke (Tucson, AZ: Univ. Arizona Press), 243
Binzel, R. P., Rivkin, A. S., Stuart, J. S., et al. 2004, Icar, 170, 259
Brozović, M., Benner, L. A. M., Taylor, P. A., et al. 2011, Icar, 216, 241
Cheng, A. F., Rivkin, A. S., Michel, P., et al. 2018, P&SS, 157, 104
de León, J., Licandro, J., Duffard, R., & Serra-Ricart, M. 2006, AdSpR, 37, 178
de León, J., Licandro, J., Serra-Ricart, M., Pinilla-Alonso, N., & Campins, H. 2010, A&A, 517, A23
Dotto, E., Della Corte, V., Amoroso, M., et al. 2021, P&SS, 199, 105185
Dunn, T. L., Burbine, T. H., Bottke, W. F., & Clark, J. P. 2013, Icar, 222, 273
Ieva, S., Dotto, E., Mazzotta Epifani, E., et al. 2018, A&A, 615, A127
Luu, J. X., & Jewitt, D. C. 1990, AJ, 99, 1985
Margot, J. L., Pravec, P., Taylor, P., Carry, B., & Jacobson, S. 2015, in Asteroids IV, ed. P. Michel et al. (Tucson, AZ: Univ. Arizona Press), 355
Michel, P., Cheng, A., Küppers, M., et al. 2016, AdSpR, 57, 2529
Michel, P., Küppers, M., & Bagatin, A. C. 2022, PSJ, 3, 160
Milliken, R. E., Hiroi, T., & Patterson, W. 2016, LPSC, 47, 2058
Monteiro, F., Rondón, E., Lazzaro, D., et al. 2021, MNRAS, 507, 5403
Moroz, L., Schade, U., & Wäsch, R. 2000, Icar, 147, 79
Perna, D., Kaňuchová, Z., Ieva, S., et al. 2015, A&A, 575, L1
Poggiali, G., Brucato, J. R., Dotto, E., et al. 2021, Icar, 354, 114040
Poggiali, G., Brucato, J. R., Hasselmann, P. H., Ieva, S., et al. 2022, PSJ, 3, 161
Popescu, M., Birlan, M., & Nedelcu, D. A. 2012, A&A, 544, A130
Pravec, P., Benner, L. A. M., Nolan, M. C., et al. 2003, IAUC, 8244, 2
Pravec, P., Thomas, C. A., & Rivkin, A. S. 2022, PSJ, 3, 175
Pravec, P., & Harris, A. W. 2007, Icar, 190, 250
Reddy, V., Dunn, T. L., Thomas, C. A., Moskovitz, N. A., & Burbine, T. H. 2015, in Asteroids IV, ed. P. Michel et al. (Tucson, AZ: Univ. Arizona Press), 43
Richardson, D. C., Barnouin, O. S., Benner, L. A. M., et al. 2016, AAS/DPS Meeting, 48, 123.17
Rivkin, A. S., Chabot, N. L., Stickle, A. M., et al. 2021, PSJ, 2, 173
Taylor, P. A. 2012, AAS/DAA Meeting, 43, 7.05
Walsh, K. J., & Jacobson, S. A. 2015, in Asteroids IV, ed. P. Michel et al. (Tucson, AZ: Univ. Arizona Press), 375
Walsh, K. J., Richardson, D. C., & Michel, P. 2008, Natur, 454, 188